Article

Self-Assembling Behavior of Amphiphilic Dendron Coils in the Bulk Crystalline and Liquid Crystalline States

Yeon-Wook Chung, Jeong-Kyu Lee, Wang-Cheol Zin, and Byoung-Ki Cho

J. Am. Chem. Soc., **2008**, 130 (22), 7139-7147 • DOI: 10.1021/ja801163m • Publication Date (Web): 03 May 2008

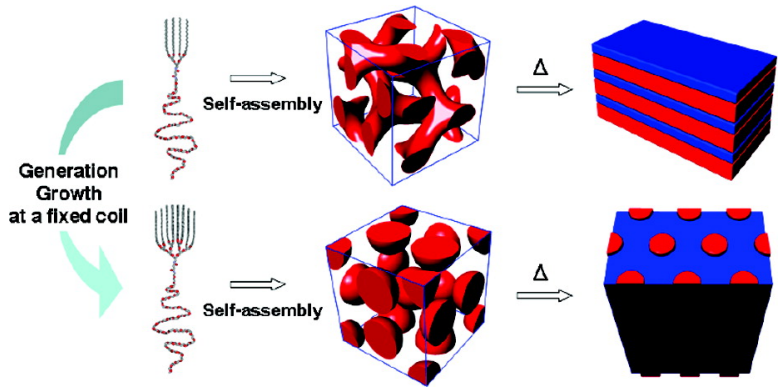

More About This Article

Additional resources and features associated with this article are available within the HTML version:

- Supporting Information
- Links to the 3 articles that cite this article, as of the time of this article download
- Access to high resolution figures
- Links to articles and content related to this article
- Copyright permission to reproduce figures and/or text from this article

View the Full Text HTML

J|A|C|S
ARTICLES

Published on Web 05/03/2008

Self-Assembling Behavior of Amphiphilic Dendron Coils in the Bulk Crystalline and Liquid Crystalline States

Yeon-Wook Chung,[†] Jeong-Kyu Lee,[‡] Wang-Cheol Zin,[‡] and Byoung-Ki Cho*,[†]

Department of Chemistry and Institute of Nanosensor and Biotechnology, Dankook University, Gyeonggi-Do, 448-701, Korea, and Department of Materials Science and Engineering, Pohang University of Science and Technology, Pohang 790-784, Korea

Received February 23, 2008; E-mail: chobk@dankook.ac.kr

Abstract: We prepared a series of amphiphilic dendron coils (**1**−**3**) containing aliphatic polyether dendrons with octadecyl peripheries and a poly(ethylene oxide) (PEO) coil (DP = 44). The molecular design in this study is focused on the variation of dendron generation (from first to third) with a fixed linear coil, upon which the thermal and self-assembling behavior of the dendron coils was investigated in the bulk. All the dendron coils exhibit two crystalline phases designated as k_1 (both crystalline octadecyl chains and PEO) and k_2 states (crystalline octadecyl chains and molten PEO). Crystallinities for both octadecyl peripheries and the PEO decrease as generation increases. In particular, the dendron coil (**3**) containing third generation shows a drastic reduction of the PEO crystallinity, which is attributed to the considerable chain folding and plasticization effects by the largest hydrophilic dendritic core segment. All the crystalline phases are bilayered lamellar morphologies. On going from k_1 to k_2, the periodic lamellar thickness decreases in the dendron coil (**1**) with first generation, but interestingly increases in **3**. After melting of octadecyl peripheries, **1** shows no mesophase (i.e., liquid crystalline phase). Additionally, dendron coil **2** (**3**) displays a network cubic mesophase with *Ia*3*d* symmetry (micellar cubic with *Pm*3*n*) which is transformed into a lamellar (hexagonal columnar) mesophase upon heating. Remarkably, the temperature-dependent mesomorphic behavior in **2** and **3** is a completely reverse pattern in comparison with conventional linear−linear block copolymers. The unusual bulk morphological phenomena in the crystalline and liquid crystalline phases can be elucidated by the dendron coil architecture and the associated coil conformational energy.

Introduction

A great deal of attention has been paid to the generation of supramolecular nanostructures by self-assembling molecules due to the tremendous potentials for the development of functional materials.[1] It has been well established that the morphological feature of each nanostructure is entirely dependent upon the identity of organizing building blocks and can be fine-tuned by the elaborate engineering of related molecular parameters such as polarity, stiffness, and architecture.[2] Therefore, a hybridization approach of architecturally distinct building blocks with their own self-assembling characteristics may become a powerful tool to develope a new class of self-assemblers.

Dendrimers/dendrons are monodisperse macromolecules with regular and highly branched architectures consisting of dendritic cores and peripheral sites. Such a peculiar structural feature provides a variety of possible applications in the field of host−guest, medicinal, and catalytic chemistries.[3] In addition, the dendrimers/dendrons have been used as a fascinating self-assembling building block.[4] The compartmentalization of chemically distinct peripheries and the dendritic core can afford to microphase-separated structures.[5] In most cases, the dendrimers/dendrons have displayed self-assembled micelles and cylinders in the bulk because of their typical cone or tapered molecular shape.

These aesthetic dendrimers/dendrons have been combined with other molecular building blocks such as rods,[6] discs,[7] or linear coils into hybrid macromolecules for the creation of new functional materials. In particular, linear coils have been compared as a counterpart with dendrimers/dendrons because of their extremely different molecular shapes, by which they reveal distinct physical properties in terms of viscosity, hydrodynamic volume, glass transition temperature, etc.[3c,8] In the last 15 years or so, because of the rapid advances in synthetic technology, an effort has been made to combine these two molecular extremes, in order to explore the role of chain topology on the physical and chemical properties. In the early stages, the aim was mostly focused on the preparation of dendritic-coil macromolecular structures by using a variety of

[†] Dankook University.
[‡] Pohang University of Science and Technology.

(1) (a) Lehn, J. M. *Supramolecular Chemistry*; VCH: Weinheim Germany, 1995. (b) Ciferri, A. *Supramolecular Polymers*, 2nd ed.; Taylor & Francis: New York, 2005. (c) Kato, T. *Science* **2002**, *295*, 2414–2418.
(2) Tschierske, C. J. *Mater. Chem.* **2001**, *11*, 2647–2671.
(3) (a) Tomalia, D. A.; Baker, H.; Dewald, J. R.; Hall, M.; Kallos, G.; Martin, S.; Roeck, J.; Ryder, J.; Smith, P. *Polym. J.* **1985**, *17*, 117–132. (b) Zeng, F. W.; Zimmerman, S. C. *Chem. Rev.* **1997**, *97*, 1681–1712. (c) Bosman, A. W.; Janssen, H. M.; Meijer, E. W. *Chem. Rev.* **1999**, *99*, 1665–1688. (d) Newkome, G. R.; He, E.; Moorefield, C. N. *Chem. Rev.* **1999**, *99*, 1689–1746.
(4) (a) Grayson, S. M.; Fréchet, J. M. J. *Chem. Rev.* **2001**, *101*, 3819–3867. (b) Hudson, H. D.; Jung, H.-T.; Percec, V.; Cho, W.-D.; Johansson, G.; Ungar, G.; Balagurusamy, V. S. K. *Science* **1997**, *278*, 449–452. (c) Gehringer, L.; Bourgogne, C.; Guillon, D.; Donnio, B. *J. Am. Chem. Soc.* **2004**, *126*, 3856–3867. (d) Fisher, M.; Vögtle, F. *Angew. Chem., Int. Ed.* **1999**, *38*, 884–905.

synthetic strategies such as anionic/living radical/ring opening polymerizations, convergent/divergent synthetic approaches, and coupling reactions.[9] More recent interest has shifted to supramolecular assembling systems applicable to material functionalities. So far, many dendritic-coil systems that self-order into nanometer-sized aggregates in a selective solvent have been reported,[10] while several examples[11] have been shown to organize into microphase-separated morphologies in the bulk state (mostly in the solid state). Among them, Meijer and coworkers reported the self-assembling behavior of dendritic-linear hybrid copolymers consisting of poly(propylene imine) dendrons functionalized with polar carboxylic acid groups and a hydrophobic linear polystyrene. They demonstrated that classical hexagonal columnar and lamellar morphologies in the solid state can be controlled as a function of dendron generation.[11a]

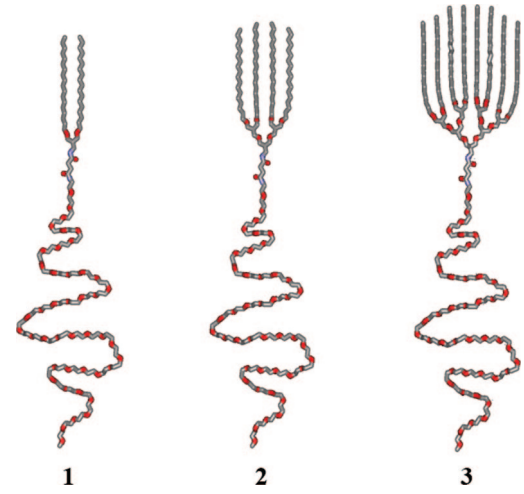

Figure 1. Molecular models of dendron coils **1**−**3**.

Hammond and co-workers used stearate-terminated poly(amidoamine) (PAMAM) dendrons as a hydrophobic head and a poly(ethylene oxide) (PEO) coil as a linear hydrophilic tail. They observed that all the copolymers exhibited lamellar structures at room temperature due to the crystallization force of the PEO coil.[11b] Nevertheless, only a few examples have displayed ordered morphologies in the melt (i.e., liquid crystalline state) as well as solid state.[12] As a representative example, Cho et al. devised amphiphilic dendron coil molecules based on third generation dendron with hydrophobic docosyl peripheries and hydrophilic linear PEO coils.[12a] They demonstrated that unique mesophase structure-mechanical and ionic transport correlations are observed by keeping the dendron generation constant while varying the length of the PEO coil.

For the engineering of crystalline and liquid crystalline morphologies in the dendron coil hybrid system, an alternative strategy is proposed utilizing variation of dendron generation at a constant linear coil length. To this end, we prepared a series of dendron coil hybrid molecules (**1**−**3**) which consist of aliphatic polyether dendrons with hydrophobic octadecyl peripheries from first to third generation and a fixed linear PEO coil with DP of 44 (Figure 1 and Scheme 1). Although the molecular design concept seems to be similar to a previous example,[11a] the enhanced incompatibility between hydrophilic and hydrophobic moieties, due to the selection of the chemically distinct molecular compositions, was capable of the study on

(5) (a) Cho, B.-K.; Jain, A.; Nieberle, J.; Mahajan, S.; Wiesner, U.; Gruner, S. M.; Türk, S.; Räder, H. J. *Macromolecules* **2004**, *37*, 4227–4234. (b) Cameron, J. H.; Facher, A.; Lattermann, G.; Diele, S. *Adv. Mater.* **1997**, *9*, 398–403. (c) Percec, V.; Cho, W.-D.; Mosier, P. E.; Ungar, G.; Yeardley, D. J. P. J. *Am. Chem. Soc.* **1998**, *120*, 11061–11070. (d) Percec, V.; Cho, W. D.; Ungar, G.; Yeardley, D. J. P. *Angew. Chem., Int. Ed.* **2000**, *39*, 1597–1602. (e) Percec, V.; Glodde, M.; Bera, T. K.; Miura, Y.; Shiyanovskaya, I.; Singer, K. D.; Balagurusamy, V. S. K.; Heiney, P. A.; Schnell, I.; Rapp, A.; Spiess, H.-W.; Hudson, S. D.; Duan, H. *Nature (London)* **2002**, *419*, 384–387. (f) Ungar, G.; Liu, Y.; Zeng, X.; Percec, V.; Cho, W. D. *Science* **2003**, *299*, 1208–1211. (g) Baars, M. W.; Söntjens, S. H. M.; Fisher, H. M.; Peerlings, H. W. I.; Meijer, E. W. *Chem.−Eur. J.* **1998**, *4*, 2456–2466. (h) Park, C.; Lee, I. H.; Lee, S.; Song, Y.; Rhue, M.; Kim, C. *Proc. Natl. Acad. Sci. U.S.A.* **2006**, *103*, 1199–1203. (i) Kim, C.; Kim, K. T.; Chang, Y.; Song, H. H.; Cho, T.-Y.; Jeon, H.-J. *J. Am. Chem. Soc.* **2001**, *123*, 5586–5587. (j) Ponomarenko, S. A.; Boiko, N. I.; Shibaev, V. P.; Richardson, R. M.; Whitehouse, I. J.; Rebrov, E. A.; Muzafarov, A. M. *Macromolecules* **2000**, *33*, 5549–5558.

(6) (a) Lee, M.; Jeong, Y.-S.; Cho, B.-K.; Oh, N.-K.; Zin, W.-C. *Chem.−Eur. J.* **2002**, *8*, 876–883. (b) Ryu, J.-H.; Kim, H.-J.; Huang, Z.; Lee, E.; Lee, M. *Angew. Chem., Int. Ed.* **2006**, *45*, 5304–5307. (c) Zubarev, E. R.; Pralle, M. U.; Sone, E. D.; Stupp, S. I. *J. Am. Chem. Soc.* **2001**, *123*, 4105–4106. (d) Zubarev, E. R.; Sone, E. D.; Stupp, S. I. *Chem.−Eur. J.* **2006**, *12*, 7313–7327.

(7) Choi, M.-S.; Aida, T.; Luo, H.; Araki, Y.; Ito, O. *Angew. Chem., Int. Ed.* **2003**, *42*, 4060–4063.

(8) Hawker, C. J.; Malmström, E. E.; Frank, C. W.; Kampf, J. P. *J. Am. Chem. Soc.* **1997**, *119*, 9903–9904.

(9) (a) Gitsov, I.; Wooley, K. L.; Hawker, C. J.; Ivanova, P. T.; Fréchet, J. M. J. *Macromolecules* **1993**, *26*, 5621–5627. (b) Gitsov, I.; Fréchet, J. M. J. *Macromolecules* **1994**, *27*, 7309–7315. (c) Leduc, M. R.; Hawker, C. J.; Dao, J.; Fréchet, J. M. J. *J. Am. Chem. Soc.* **1996**, *118*, 11111–11118. (d) Zhu, L.; Tong, X.; Li, M.; Wang, E. *J. Polym. Sci., Part A: Polym. Chem.* **2000**, *38*, 4282–4288. (e) Zhao, Y.-L.; Jiang, J.; Liu, H.-W.; Chen, C.-F.; Xi, F. *J. Polym. Sci., Part A: Polym. Chem.* **2001**, *39*, 3960–3966. (f) Mecerreyes, D.; Dubois, P. H.; Jérôme, R.; Hendrick, J. L.; Hawker, C. J. *J. Polym. Sci., Part A: Polym. Chem.* **1999**, *37*, 1923–1930. (g) Connal, L. A.; Vestberg, R.; Hawker, C. J.; Qiao, G. G. *Macromolecules* **2007**, *40*, 7855–7863. (h) Emrick, T.; Hayes, W.; Fréchet, J. M. J. *J. Polym. Sci., Part A: Polym. Chem.* **1999**, *37*, 3748–3755. (i) Al-Muallem, H. A.; Knauss, D. M. *J. Polym. Sci., Part A: Polym. Chem.* **2001**, *39*, 152–161. (j) Froimowicz, P.; Paez, J.; Gandini, A.; Belgacem, N.; Strumia, M. *Macromol. Symp.* **2006**, *245−246*, 51–60.

(10) (a) Chapman, T. M.; Hillyer, G. L.; Mahan, E. J.; Shaffer, K. A. *J. Am. Chem. Soc.* **1994**, *116*, 11195–11196. (b) van Hest, J. C. M.; Delnoye, D. A. P.; Baars, M. W. P. L.; Van Genderen, M. H. P.; Meijer, E. W. *Science* **1995**, *268*, 1592–1595. (c) van Hest, J. C. M.; Baars, M. W. P. L.; Elissen-Román, C.; van Genderen, M. H. P.; Meijer, E. W. *Macromolecules* **1995**, *28*, 6689–6691. (d) Iyer, J.; Fleming, K.; Hammond, P. T. *Macromolecules* **1998**, *31*, 8757–8765. (e) Iyer, J.; Hammond, P. T. *Langmuir* **1999**, *15*, 1209–1306. (f) Chang, Y.; Kwon, Y. C.; Lee, S. C.; Kim, C. *Macromolecules* **2000**, *33*, 4496–4500. (g) Aoi, K.; Motoda, A.; Okada, M.; Imae, T. *Macromol. Rapid Commun.* **1997**, *18*, 945–952. (h) Barriau, E.; Marcos, A. G.; Kautz, H.; Frey, H. *Macromol. Rapid Commun.* **2005**, *26*, 862–867. (i) Ge, Z.; Luo, S.; Liu, S. *J. Polym. Sci., Part A: Polym. Chem.* **2006**, *44*, 1357–1371. (j) Gillies, E. R.; Jonsson, T. B.; Fréchet, J. M. J. *J. Am. Chem. Soc.* **2004**, *126*, 11936–11943. (k) Tian, L.; Hammond, P. T. *Chem. Mater.* **2006**, *18*, 3976–3984.

(11) (a) Román, C.; Fischer, H. R.; Meijer, E. W. *Macromolecules* **1999**, *32*, 5525–5531. (b) Johnson, M. A.; Iyer, J.; Hammond, P. T. *Macromolecules* **2004**, *37*, 2490–2501. (c) Mackay, M. E.; Hong, Y.; Jeong, M.; Tande, B. M.; Wagner, N. J.; Hong, S.; Gido, S. P.; Vestberg, R.; Hawker, C. J. *Macromolecules* **2002**, *35*, 8391–8399. (d) Pochan, D. J.; Pakstis, L.; Huang, E.; Hawker, C.; Vestberg, R.; Pople, J. *Macromolecules* **2002**, *35*, 9239–9242. (e) Magbitang, T.; Lee, V. Y.; Cha, J. N.; Wang, H.-L.; Chung, W. R.; Miller, R. D.; Dubois, G.; Volksen, W.; Kim, H.-C.; Hedrick, J. L. *Angew. Chem., Int. Ed.* **2005**, *44*, 7574–7580. (f) Duan, X.; Yuan, F.; Wen, X.; Yang, M.; He, B.; Wang, W. *Macromol. Chem. Phys.* **2004**, *205*, 1410–1417. (g) Gao, Y.; Zhang, X.; Yang, M.; Zhang, X.; Wang, W.; Wegner, G.; Burger, C. *Macromolecules* **2007**, *40*, 2606–2612.

(12) (a) Cho, B.-K.; Jain, A.; Gruner, S. M.; Wiesner, U. *Science* **2004**, *305*, 1598–1601. (b) Cho, B.-K.; Jain, A.; Gruner, S. M.; Wiesner, U. *Chem. Commun.* **2005**, 2143–2145. (c) Cho, B.-K.; Jain, A.; Gruner, S. M.; Wiesner, U. *Chem. Mater.* **2007**, *19*, 3611–3614. (d) Kim, J.-K.; Hong, M.-K.; Ahn, J.-H.; Lee, M. *Angew. Chem., Int. Ed.* **2005**, *44*, 328–332.

(13) Chung, Y.-W.; Lee, B.-I.; Kim, H.-Y; Wiesner, U.; Cho, B.-K. *J. Polym. Sci. Part A: Polym. Chem.* **2007**, *45*, 4988–4994.

Scheme 1. Synthesis of Dendron Coils **1**−**3**

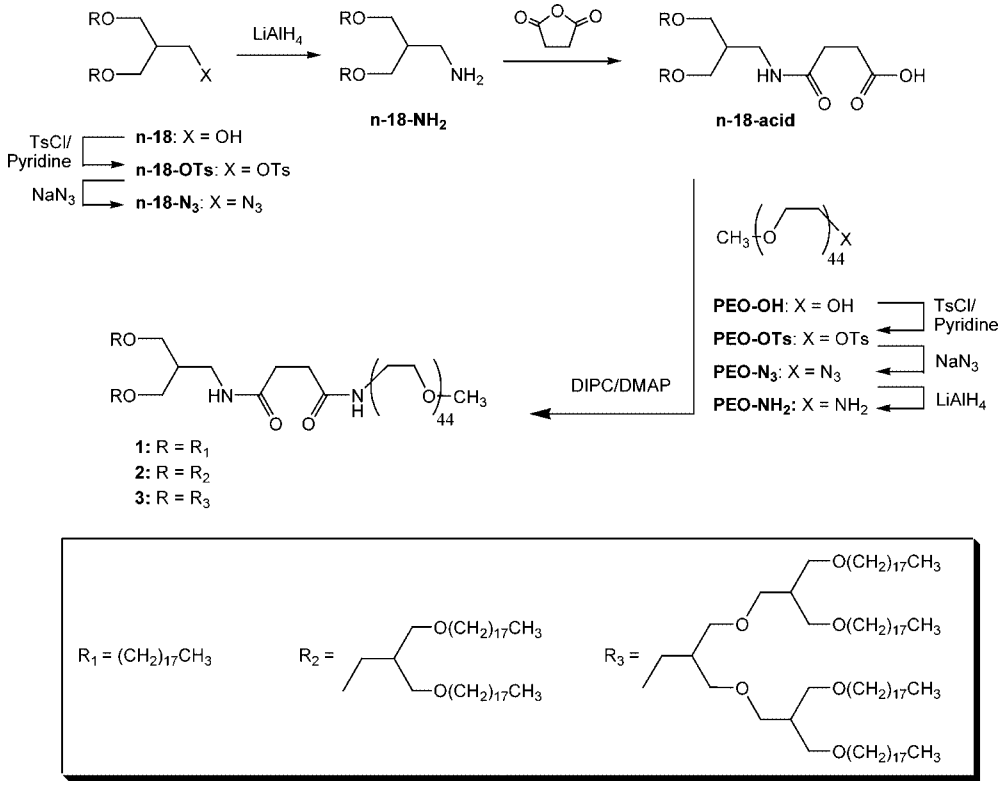

Table 1. Characterization of Dendron Coils **1**−**3**

dendron coil	M_n (g/mol)		PDI (M_w/M_n)	hydrophilic volume fraction (f_v)	phase transitions (°C) and corresponding enthalpy changes (J/g)	crystallinity[h]	
	^{1}H NMR	MALDI-TOF MS				PEO	octadecyl
1	2659.84	2512.20	1.01[a]−1.04[b]	0.75[c]−0.77[d]	k_1 51.8 (104.3)[e] k_2 73.2 (52.1)[e] i	0.75	0.93
2	3340.51	3249.13	1.00[a]−1.05[b]	0.62[c]−0.64[d]	k_1 45.0 (76.8)[e] k_2 52.6 (43.1)[e] nc 62.0[f] lam 92.3[g] i	0.70	0.49
3	4701.85	4591.16	1.00[a]−1.04[b]	0.49[c]−0.51[d]	k_1 23.9 (27.4)[e] k_2 49.5 (57.9)[e] mc 77.0[f] col 102.1[g] i	0.35	0.46

[a] From MALDI-TOF MS. [b] From GPC. [c] k_1 phase. [d] Melt state. [e] Second heating data from DSC. [f] From SAXS. [g] From DMS. [h] Crystallinity = experimental heat of fusion of a sigle PEO (octadecyl group)/heat of fusion of a perfect crystalline PEO (octadecyl group). Experimental heat of fusion of a PEO(octadecyl group) (kJ/mol) = heat of fusion (J/g) from DSC × mass of a PEO (octadecyl group)/weight fraction. The heat of fusion of a single perfect crystalline PEO (octadecyl group) was calculated on the basis of the heat of fusion of a repeat unit in the perfect crystalline of 8.4 kJ/mol (4.11 kJ/mol). k = crystalline, nc = network cubic, lam = lamellar, mc = micellar cubic, col = hexagonal columnar, i = isotropic liquid.

the self-assembling behavior in both liquid crystalline (i.e., mesophase) and solid phases.

In this paper, we report on the details of synthesis, and the thermal and self-assembling properties of dendron coils **1**−**3**, providing insight on the correlation between chain topology and physical properties, and a molecular design concept for the creation of a new class of self-assembling soft materials. In particular, unprecedented findings in crystalline and liquid crystalline assemblies as a function of dendron generation or temperature, for example, crystalline lamellar dimensional variation and temperature-dependent phase transition, are described.

Results and Discussion

Synthesis. The synthetic procedure is outlined in Scheme 1. The synthesis of the dendrons (**n-18**) from first to third generation containing aliphatic polyether dendritic cores and octadecyl peripheries was performed via a convergent synthetic method consisting of a Williamson etherification and hydroboration/oxidation reactions.[13,14] As a fixed hydrophilic coil, we employed a poly(ethylene glycol) methyl ether with average molecular weight of 2000 g/mol from Aldrich Corp. As measured by ^{1}H NMR spectroscopy, the average number of repeating units (DP = 44) in the PEO of the dendron coils determined from the ratio of the four protons next to the carbonyl groups to the ethylene protons of the PEO backbone, was almost identical to the value of DP = 45 assigned by the chemical supplier. The number average molecular weights (M_n) in Table 1 were calculated on the basis of the NMR measurements. The hydroxyl ends of both the dendron and the PEO coil were converted into amine groups by the following reaction sequence; (i) tosylation by tosyl chloride, (ii) azidation by sodium azide, and (iii) reduction by lithium aluminum hydride. Most of the reaction steps were performed in good yields above 70%. For the coupling of the dendron and coil segments, each dendron generation was functionalized with a carboxylic acid end group by reacting with excess succinic anhydride. The final coupling reaction of carboxylic acid terminated dendrons (**n-**

(14) Jayaraman, M.; Fréchet, J. M. J. *J. Am. Chem. Soc.* **1998**, *120*, 12996–12997.
(15) Grason, G. M.; DiDonna, B. A.; Kamien, R. D. *Phys. Rev. Lett.* **2003**, *91*, 58304.

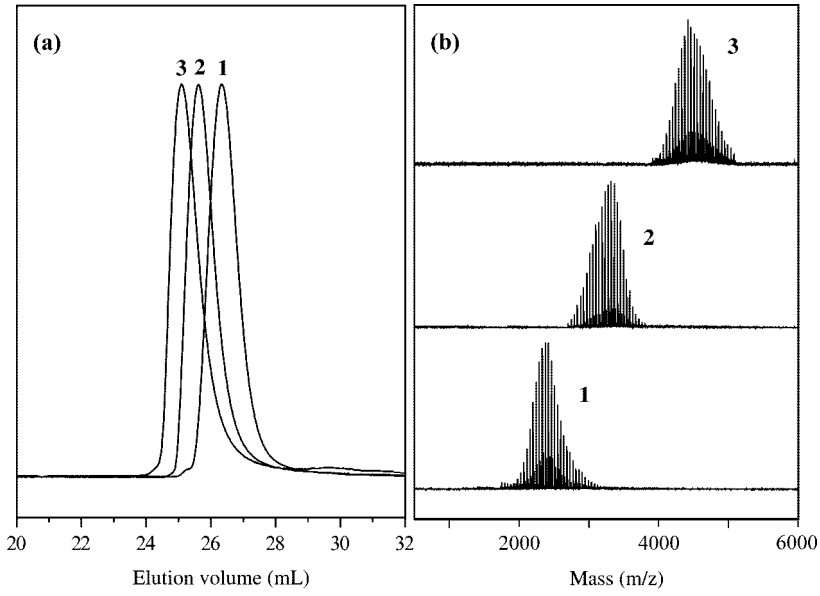

Figure 2. (a) GPC curves and (b) MALDI-TOF mass spectra of **1**−**3**.

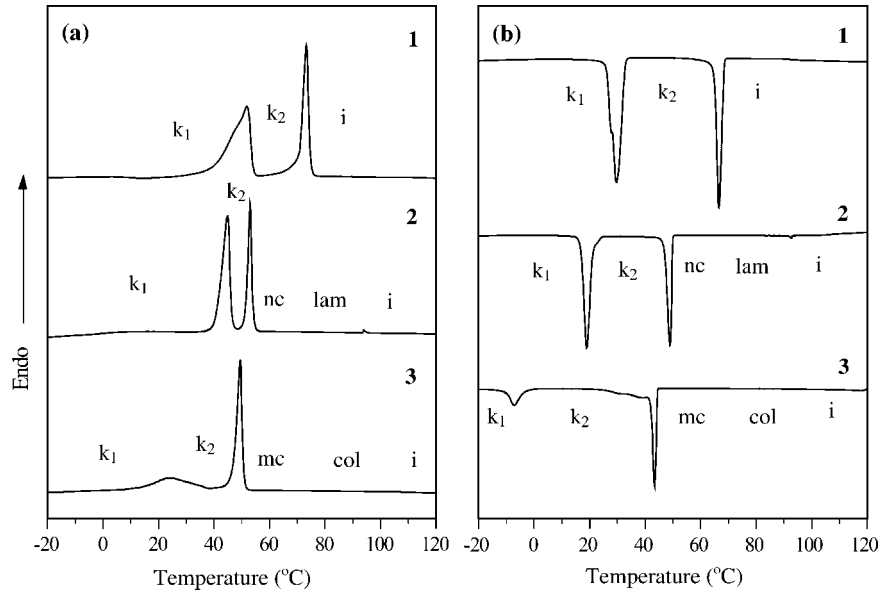

Figure 3. DSC thermograms of **1**−**3** from (a) second heating and (b) first cooling scans.

18-acid) and amine terminated PEO was performed using *N*,*N*′-diisopropylcarbodiimide in the presence of 4-dimethylaminopyridine.

The resulting dendron coil molecules (**1**−**3**) were characterized by ^{1}H NMR and matrix-assisted laser desorption ionization time-of-flight mass spectrometry (MALDI-TOF MS), elemental analysis (EA) and gel permeation chromatography (GPC). All dendron coils show narrow polydispersities (M_w/M_n) of less than 1.05 in GPC (Figure 2a and Table 1), and exhibit signals for the α-protons to the carbonyl groups at 2.56 ppm. Elemental analysis data of **1**−**3** are also in good agreement with the theoretical values.

Figure 2b is the MALDI-TOF mass spectra of **1**−**3**. The M_n values of **1**−**3** were estimated to be 2512, 3249, and 4591 g/mol, respectively. Theses molecular weights are consistent with the M_n values determined from the NMR measurement within a 5% error range. In addition, their polydispersities from MALDI-TOF MS are less than 1.01, indicative of high purity (Table 1).

Thermal Characterization. The thermal behavior of **1**−**3** was studied by differential scanning calorimetry (DSC), temperature dependent small-angle X-ray scattering (SAXS), and dynamic mechanical spectroscopy (DMS). The results are summarized in Table 1. As shown in Figure 3, the DSC thermograms of **1**−**3** display two melting transitions which can be observed reversibly on both heating and cooling scans. Considering the molecular compositions, the melting transitions observed at the lower and higher temperatures correspond to the meltings of the crystalline PEO coil and octadecyl peripheral chains, respectively. Both melting transition temperatures decrease on going from **1** to **3**. This phenomenon might be attributed to the reduction of crystalline parts in both alkyl and PEO regions as the dendron generation increases. Table 1 presents the degrees of crystallinity in both melting transitions for **1**−**3**. The values can be determined by comparing the heats of fusion on the second heating to that of a perfect crystalline octadecyl chain (PEO coil). For octadecyl peripheries, the crystallinity decreases

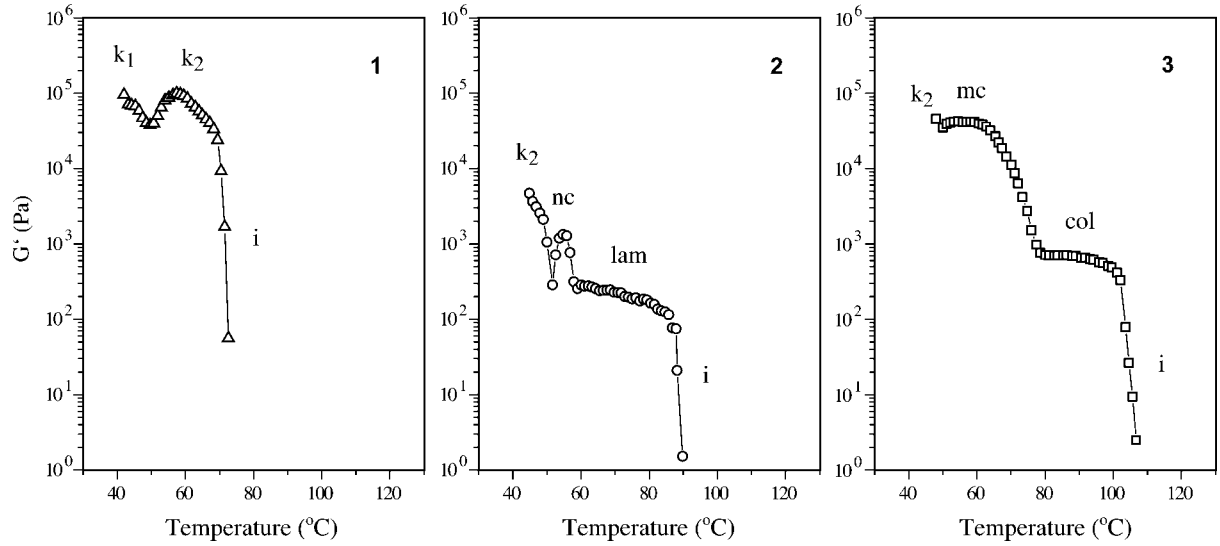

Figure 4. Elastic modulus G' as a function of temperature for dendron coils **1**−**3**.

from 93, 49, to 46% with increasing dendron generation. We conjecture that the reduction is strongly dependent on the variation of intrinsic curvature with each generation. The interface between peripheral groups and dendritic core would be more curved with increasing generation number because of the starburst molecular shape, which decreases the packing area of octadecyl peripheries, resulting in the reduction of crystallinity. Also, the PEO crystallinity decreases as generation increases. Particularly, a significant reduction from 70 to 35% occurs between **2** and **3**. This might be predominantly caused by the degree of chain folding in PEO crystals depending on dendron size. Because the dendron cross section of **3** is the largest, the PEO crystals formed by **3** may contain the largest folding defect, resulting in the reduction of crystallinity. In addition, a plasticization of PEO coils by amorphous dendritic cores can influence the crystallinity to some extent.[9a] Since the basic repeating unit of aliphatic polyether dendritic cores, that is, $CH_2CH(CH_2O)_2$, is almost identical to a doubled poly(ethylene oxide) structural unit: $2 \times (CH_2CH_2O)$, it is probable that the dendritic cores plasticize the crystalline linear PEO coils. The size of aliphatic polyether dendritic cores increases by a factor of 2 with each generation, therefore both chain folding and plasticization effects are expected to be maximized in **3**, rationalizing the precipitous reduction of PEO crystallinity in **3**.

Meanwhile, phase transitions in the melt were difficult to observe in the DSC data. Our dendron coils consist of fully aliphatic chains, thus the associated energy to phase transitions such as mesophase-to-mesophase/mesophase-to-liquid, might be too small to be identified by DSC. However, the phase transitions are accompanied by detectable mechanical change, for example, elastic modulus (G'). Therefore, the transitions were able to be monitored by DMS measurements (Figure 4). As determined by combination of temperature variable SAXS data, the phase transitions in the melt are summarized in Table 1.

Self-Assembly in the Crystalline k_1 and k_2 Phases. To investigate the microstructures in the crystalline and liquid crystalline phases, SAXS experiments have been performed with the dendron coils at various temperatures. The SAXS patterns of all the dendron coils in k_1 and k_2 phases display multiple reflections with q-spacing ratios of 1:2:3..., indicative of lamellar structures (Figure 5). From the observed primary peak, *d*-spacings in the crystalline phases were estimated and summarized in Table 2.

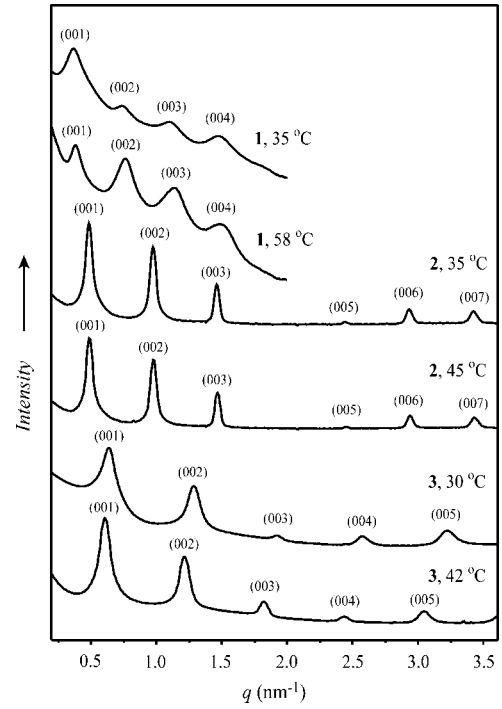

Figure 5. SAXS patterns of **1**−**3** in k_1 and k_2 phases.

Table 2. Characterization of Dendron Coils **1**−**3** by Small-Angle X-Ray Scattering[a]

	crystalline		liquid crystalline			
dendron coil	k_1 - lamellar *d*-spacing (nm)	k_2 - lamellar *d*-spacing (nm)	*ia3d* *a* (nm)	lamellar *d*-spacing (nm)	*Pm3n* *b* (nm)	hexagonal columnar *c* (nm)
1	17.03	16.38				
2	12.90	12.90	21.32	7.47		
3	9.78	10.01			20.49	9.25

[a] *a*, *b*, and *c* are the lattice constants of the structures.

For the details of packing structure, we can assume that the molecular section of a single molecule is a square column in the lamellar structure. On the basis of that assumption and the

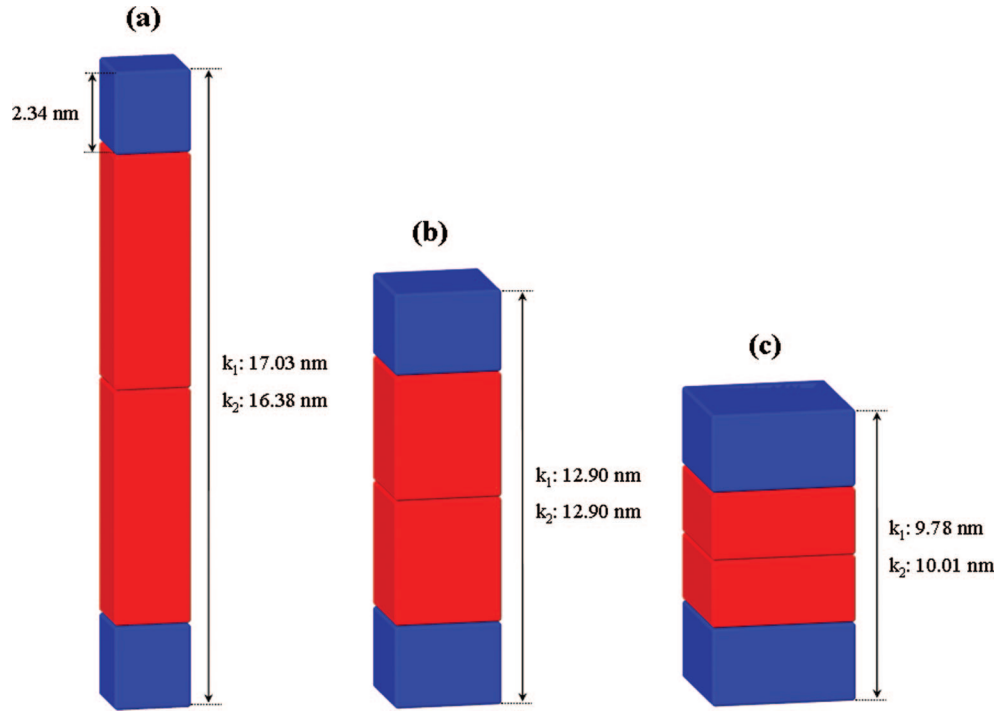

Figure 6. Molecular sections of (a) **1**, (b) **2**, and (c) **3** in the bilayered crystalline phases; the blue and red colors represent the hydrophobic and hydrophilic parts, respectively.

fully stretched octadecyl chain length of 2.34 nm from CPK model, the lengths of the molecular sections were calculated to be 8.79, 5.83, and 4.33 nm for **1**−**3**, respectively. The decrease of the calculated molecular sectional length from **1** to **3** is quite reasonable because the cross sectional area of the molecular section increases proportionally with dendron generation. When the molecular sectional length is compared with the lamellar *d*-spacing, the latter is approximately twice of the former. Therefore, it can be concluded that the dendron coils form bilayered lamellar structures in k_1 and k_2 crystalline phases (Figure 6).

Additionally, it is interesting to note the subtle *d*-spacing change between k_1 and k_2 in **1**−**3**. When comparing between k_1 and k_2, the lamellar *d*-spacing slightly decreases in **1**, but somewhat increases in **3**. We speculate that this reverse trend between **1** and **3** is attributed to the variation of conformation energy and density of PEO coils upon melting of PEO coils. In contrast to k_1 where PEO coils are crystalline, PEO coils in k_2 are molten. Therefore, the conformational energy of PEO coils in k_2 is closely dependent upon the shape of the space occupied by them in the bilayered lamellar structure. As shown in Figure 6, the PEO space becomes isotropic as the dendron generation increases, thus we can expect that the PEO conformational energy (i.e., stretching penalty) would be the highest in **1** and the lowest in **3**. In this regard, one way to reduce the PEO conformational energy in **1** might be a slight lateral expansion of linear coil conformation, although at the present moment we are not aware of how to change the octadecyl packing. Consequently, the overall *d*-spacing in k_2 may be estimated to be slightly smaller than that in k_1. On the contrary, the PEO section of **3** in k_1 would be relatively isotropic to adopt more random coil-like conformations. In this situation, the increased PEO volume upon melting of the PEOs might lead to the slight increase of the overall *d*-spacing. In intermediate dendron coil **2**, we assume that no change in the *d*-spacing was observed as a result of the compensation of these two factors.

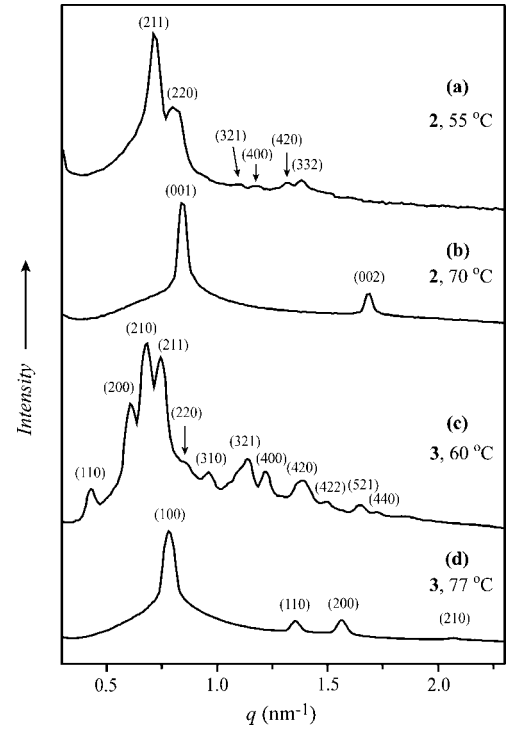

Figure 7. SAXS patterns of **2** and **3** in the liquid crystalline phases.

Characterization of the Liquid Crystalline Phases of 2 and 3. As supported by the DMS data, upon melting of the octadecyl peripheries dendron coils **2** and **3** show two liquid crystalline phases (mesophases) before disordering into an isotropic liquid at 92.3 and 102.1 °C, respectively. The microstructures were characterized by a temperature-dependent SAXS technique. In Figure 7a, the SAXS pattern of **2** at 55 °C exhibits multiple reflections with *q*-spacing ratios of $\sqrt{6}$:$\sqrt{8}$:$\sqrt{14}$:$\sqrt{16}$:$\sqrt{20}$:$\sqrt{22}$.

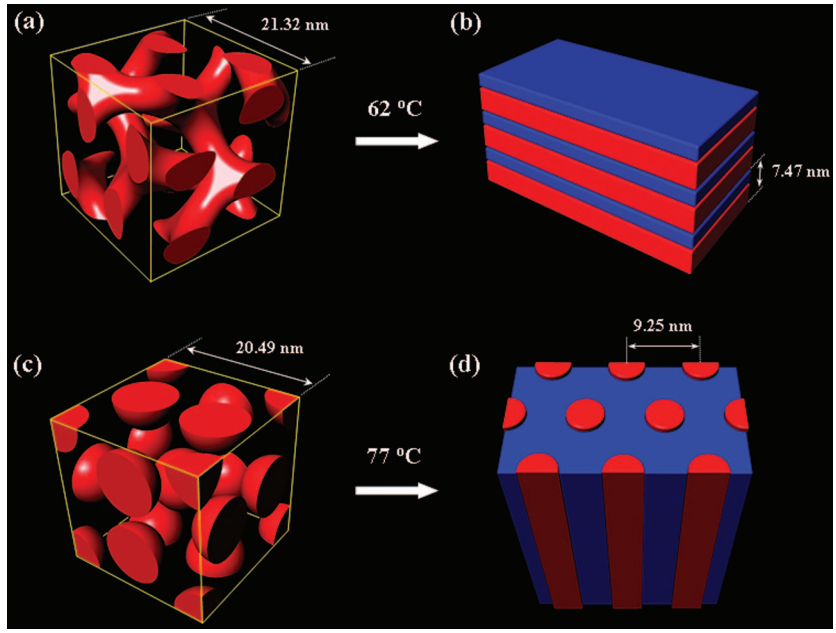

Figure 8. Schematic sketches of (a) network cubic (*Ia3d* symmetry), (b) lamellar, (c) micellar cubic (*Pm3n* symmetry), and (d) hexagonal columnar mesophases of dendron coils **2** (a,b) and **3** (c,d). The blue and red colors represent the hydrophobic and hydrophilic regions, respectively. For reasons of clarity, the hydrophobic matrix is omitted in (a) and (c).

These peaks can be indexed as the (211), (220), (321), (400), (420), and (332) reflections of a cubic structure with *Ia3d* symmetry (Table S1, Supporting Information). From the observed *d*-spacing of (211) reflection, the best fit value for the cubic lattice parameter is 21.32 nm (Figure 8a). Upon further heating, **2** displays two reflections with a *q*-spacing ratio of 1:2 at 70 °C, indicating a lamellar mesophase with a periodic thickness of 7.47 nm (Figures 7b and 8b).

As compared with the *d*-spacing of 12.90 nm in the crystalline lamellar phases, the periodic thickness in the lamellar mesophase suggests a fundamental change in the molecular organization. Assuming the length of a stretched octadecyl group to be 2.34 nm, the ratio of the hydrophilic layer thickness (5.13 nm) with respect to the *d*-spacing (7.47 nm) is 0.68 which is approximately identical to the hydrophilic volume fraction of 0.64. Since molecular volumes are linearly proportional to *d*-spacing in lamellar structures, this strongly suggests that the dendron segments in the lamellar mesophase self-assemble into an interdigitated monolayer (Figure S1, Supporting Information). The change in the arrangement of peripheral chains from a bilayer to an interdigitated monolayer may relieve the conformation of flexible PEO coils in the molten state by enlarging the cross-sectional area.

For dendron coil **3**, with the largest third generation, a cubic morphology is detected after melting of the peripheries. In Figure 7c, the SAXS pattern at 60 °C exhibits a considerably larger number of reflections which can be indexed as the (110), (200), (210), (211), (220), (310), (321), (400), (420), (422), (521), and (440), indicative of a *Pm3n* cubic symmetry (Table S2, Supporting Information). From the dimension of the (200) reflection, the cubic lattice parameter can be estimated as 20.49 nm (Figure 8c). Upon further heating, the SAXS pattern changes into four reflections with *q*-spacing ratios of $1:\sqrt{3}:\sqrt{4}:\sqrt{7}$ which is characteristic of a 2-D hexagonal columnar structure (Figures 7d and 8d). The lattice constant is determined to be 9.25 nm.

The observed phase sequence as a function of dendron generation, that is, *Ia3d* cubic/lamellar for **2** and *Pm3n* cubic/columnar for **3**, suggests that the *Ia3d* and *Pm3n* cubic phases are continuous network and discrete micellar morphologies, respectively. Furthermore, a recent theoretical approach demonstrated that a micellar cubic phase with *Pm3n* symmetry exists over a relatively large volume fraction range in dendritic-linear hybrid block systems.[15] On the basis of these results, it should be noted that the molecular approach proposed in this study, that is, *a simple variation of dendron generation at a fixed linear coil*, provides a versatile way to engineer lamellar crystalline and a variety of liquid crystalline phases including micellar, columnar, lamellar, continuous cubic structures.

Temperature-Dependent Phase Behavior. Besides the rich phase behavior, the most notable feature of the dendron coils is the unusual temperature-dependent phase sequence in the melt states of **2** and **3**. On melting of octadecyl peripheries, dendron coil **2** displays a network cubic mesophase which is transformed into a lamellar mesophase. Likewise, dendron coil **3** displays a micellar cubic mesophase, which is transformed into a hexagonal columnar mesophase. These phase sequences are quite unusual in comparison with other block copolymers, which show a completely reverse phase sequence. As temperature increases, conventional block copolymers with linear-linear architecture have been known to conform to the following phase sequence; from lamellar, continuous network cubic, hexagonal columnar to micellar cubic mesophases in the melt.[16] The remarkable contrast between our dendron coils and other block copolymers might be originated from their polymeric chain architectures. In conventional block copolymers with linear-linear components, for a given microstructure with a curved interface (e. g., columnar or micellar), a linear block with a larger volume fraction (or longer coil length) tends to be located in the outer

(16) (a) Hamley, I. W. *The Physics of Block Copolymers*; Oxford Univ. Press: New York, 1998. (b) Hillmyer, M. A.; Bates, F. S.; Almdal, K.; Mortensen, K.; Ryan, A. J.; Fairclough, J. P. A. *Science* **1996**, *271*, 976–978.

(17) (a) Frischknecht, A.; Fredrickson, G. H. *Macromolecules* **1999**, *32*, 6831–6836. (b) Pickett, G. T. *Macromolecules* **2002**, *35*, 1896–1904. (c) Grason, G. M. *Phys. Rep.* **2006**, *433*, 1–64.

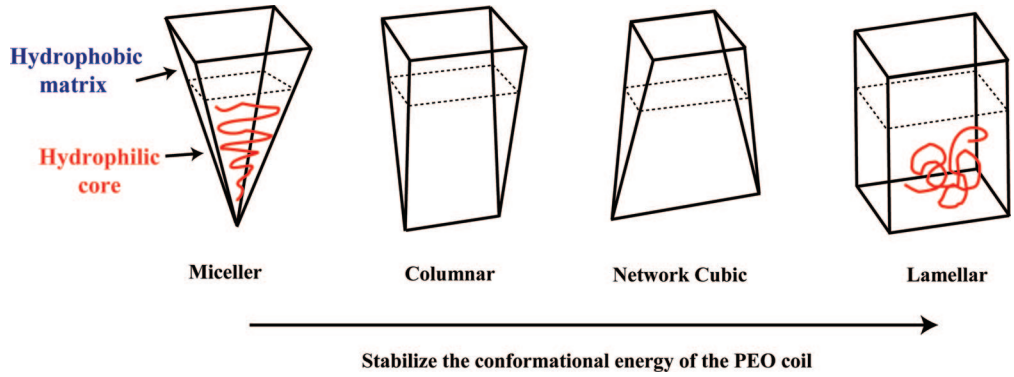

Figure 9. Molecular sections in various morphologies. In the dendron coil system, it is expected that the bulky hydrophobic peripheries are located in the outer matrix, on the other hand the hydrophilic PEO coil occupies inner core.

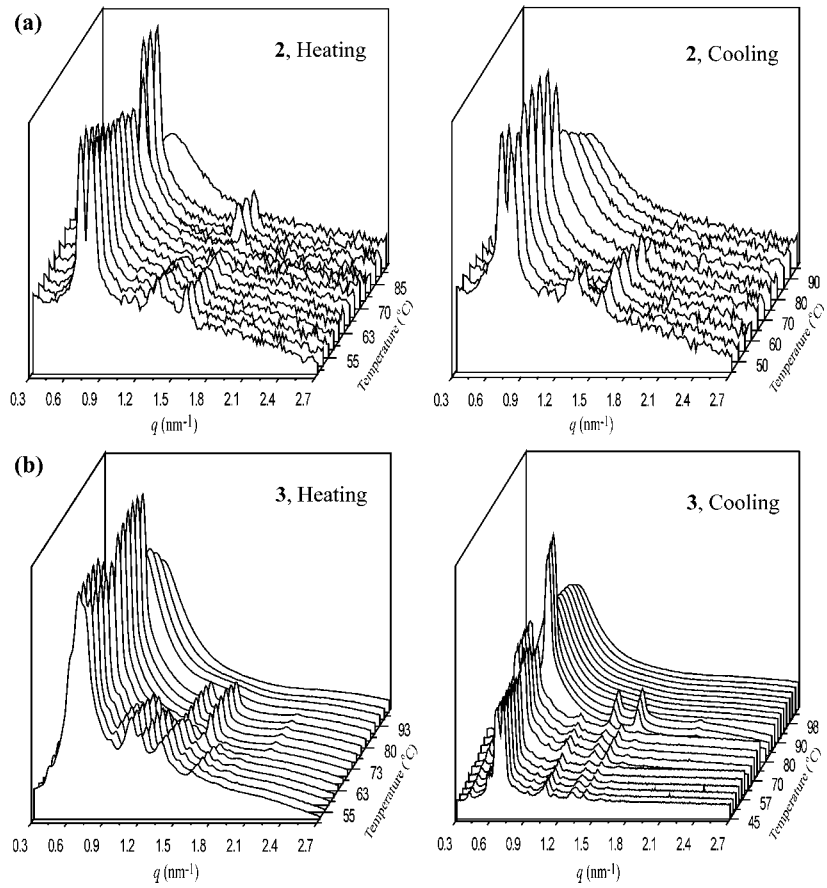

Figure 10. SAXS data for (a) **2** and (b) **3** on heating and cooling scans.

matrix, while the other linear block with the smaller volume fraction occupies the inner core. Through such a location, the longer coil is able to adopt more stable conformations like a random coil, which relieves the overall conformational energy. To this end, the phase diagram of the linear-linear block copolymer system shows an approximately symmetric shape, although the asymmetry factor between the blocks distorts the phase diagram to some extent.

In contrast, the dendron coil molecules are composed of architecturally distinct dendron and linear segments. From this structural feature, despite the smaller hydrophobic volume fractions the bulky peripheries are favored in the outer matrix, in order to reduce the steric hindrance. In this configuration, the curved interface relaxes the peripheral octadecyl chains at the expense of an increased stretching penalty of the PEO chain.[17] By considering the fact that the hydrophobic peripheries occupy the outer matrix, despite the major hydrophilic volume fractions of **2** and **3** (i.e., 0.64 and 0.51), it is suggested that the phase boundaries in the present dendron coil system are significantly shifted toward larger volume fractions of the hydrophilic part when compared to conventional linear-linear block copolymers. As the temperature elevates, however, the conformational energy of the PEO coil in the inner core would be increased because the conformational state of the longer PEO chain is more than that of the octadecyl chain. Therefore, at higher temperatures the morphology should change to a different morphology, one which can alleviate the stretching penalty of the PEO chain. By comparing the interfacial curvature of the

(18) Milner, S. T. *Macromolecules* **1994**, *27*, 2333–2335.

network cubic (micellar cubic) structure with that of the lamellar (hexagonal columnar) structure, the former would be larger than the latter. This reduction of the interfacial curvature seems very surprising when compared to linear-linear block copolymers, but in our dendron coil system where the phase inversion hardly occurs, this curvature change is quite plausible. Here, it would be useful to take into account the molecular sections in the various morphologies presented by Milner (Figure 9).[18] As the morphology moves from micellar to lamellar structures, the inner coil conformation becomes more isotropic, which allows the linear coil to adopt more random coil-like conformations. Thus, this consideration clearly explains the unique mesophase transformation upon heating in our dendron coil system.

It is also important to stress the fact that the observed phase transitions take place in completely reversible fashion on both heating and cooling scans, as evidenced by the SAXS data (Figures 10). Frey et al. reported a similar phase transition from hexagonal columnar to lamellar structures on heating in their dendritic poly(carbosilane)-*b*-linear polystyrene copolymers.[19] However, the hexagonal columnar structure observed at lower temperatures was revealed as a metastable phase which transforms into the lamellar structure when annealed. In this regard, the reversibility of phase transition in our system is quite unique.

Conclusions

We prepared a series of amphiphilic dendron coils **1**-**3** consisting of aliphatic polyether dendrons with hydrophobic octadecyl peripheries and a hydrophilic linear PEO coil. For the engineering of a variety of crystalline and liquid crystalline morphologies in the bulk, a molecular design approach, that is, variation of the dendron generation from first to third at a fixed PEO coil, was employed. All the dendron coils show two crystalline phases k_1 and k_2 which turned out to be bilayered lamellar morphologies. Interestingly, on transitioning from k_1 to k_2, the lamellar *d*-spacing changes in different ways depending on the dendron coils. The *d*-spacing decreases in dendron coil **1**, while the *d*-spacing of **3** in the k_2 is a bit larger that that in the k_1. After the melting of octadecyl peripheries, no mesophase was observed in dendron coil **1**. On the other hand, **2** and **3** were shown to self-assemble into two different kinds of mesophases as a function of temperature, respectively. As convinced by SAXS data, upon heating **2** spontaneously organizes a network cubic mesophase (nc) with *Ia*3*d* symmetry, which is transformed into a lamellar mesophase (lam). In dendron coil **3**, it has been proven that a micellar cubic mesophase (mc) with *Pm*3*n* symmetry turns into a hexagonal columnar mesophase (col) as temperature increases. Despite the observed rich phase behavior, the most remarkable feature in this study is the temperature dependent phases sequence; the transformations as a function of temperature are quite unusual in comparison to conventional linear-linear block copolymers which have shown the reverse phase sequence, for example, lam-to-nc/col-to-mc. The reversibility of the transformations is another unique characteristic as compared to a similar transition observed in linear-hyperbranched block copolymers. Consequently, the molecular design concept proposed in this study demonstrated that a variety of morphologies and unusual phase transformations in the bulk crystalline and liquid crystalline phases can be tuned as a function of dendron generation/or temperature, and furthermore, may provide a versatile strategy for nanostructured functional soft materials.

Acknowledgment. This work was supported by the Korea Science and Engineering Foundation (R01-2006-000-11221-0), Korea Research Foundation (D00069), and a grant from the Fundamental R&D Program for Core Technology of Materials funded by the Ministry of Commerce, Industry and Energy, Republic of Korea. We acknowledge Pohang Accelerator Laboratory (Beamline 10C1), Korea.

Supporting Information Available: Experimental sections; Tables S1 and S2; Figure S1. This material is available free of charge via the Internet at http://pubs.acs.org.

JA801163M

(19) Marcos, A. G.; Pusel, T. M.; Thomann, R.; Pakular, T.; Okrasa, L.; Geppert, S.; Gronski, W.; Frey, H. *Macromolecules* **2006**, *39*, 971–977.